

Structure of the Nucleon Spin on the Light Cone

B. Pasquini

*Dipartimento di Fisica Nucleare e Teorica, Università degli Studi di Pavia, and
Istituto Nazionale di Fisica Nucleare, Sezione di Pavia, I-27100 Pavia, Italy*

Abstract. The spin structure of the nucleon is studied in a light-cone description of the nucleon where the Fock expansion is truncated to consider only valence quarks. Transverse momentum dependent parton distributions and transverse-spin densities, defined through the generalized parton distributions in the impact parameter space, are investigated as new tools to reveal the spin-spin and spin-orbit correlations for different quark and nucleon polarizations.

Keywords: Parton correlation functions, nucleon spin, light-cone quantization

PACS: 12.39.Ki, 13.85.Ni, 13.60.-r

INTRODUCTION

One of the most important goal in QCD spin physics is to understand the spin structure of the nucleon, i.e. how the nucleon spin is made from its fundamental constituents. This issue has been of intensive experimental and theoretical investigation over the last decades, in particular by exploring the QCD parton model in deep inelastic processes in terms of unpolarized and helicity parton distributions functions (PDFs). In recent years a precise knowledge of the transverse structure as well as of parton-momentum correlations has emerged as an essential part to unravel the spin and momentum substructure of the nucleon. This information can only be obtained by considering processes beyond the inclusive reactions, such as semi-inclusive deep-inelastic (SIDIS) lepton nucleon scattering or exclusive lepto-production processes at large momentum transfer. According to the factorization theorem, the physical observables of such processes can be expressed as convolution of hard partonic scattering cross sections, and soft non-perturbative objects given by quark-quark correlation functions which generalize the forward matrix elements occurring in the definition of the PDFs. In the case of SIDIS processes one deals with transverse momentum dependent parton distributions (TMDs) which are defined in terms of the same matrix elements entering the definition of PDFs, but without integration over the transverse momentum [1]. On the other hand, exclusive processes such as $eN \rightarrow eN\gamma$ or $eN \rightarrow eNM$ (where $M = \pi, \rho, K$ etc.) allow to access generalized parton distributions (GPDs) which involve non-forward matrix elements between hadron states with different momentum and/or polarization before and after the scattering [2]. Although the TMDs and GPDs can be seen as two different limiting cases of the same generalized parton correlation functions, no-model independent relations between the two classes of objects has been obtained so far [3].

The TMDs contain rich and direct three-dimensional information about the internal dynamics of the nucleon, and in particular can help in understanding the strength of different spin-spin and spin-orbit correlations. On the other hand, the GPDs provide new

method of spatial imaging of the nucleon, through the definition of impact-parameter dependent spin densities which reveal the correlations between the momentum and spatial distributions of quarks for different quark and target polarizations. A convenient way to make explicit which kind of information on hadron structure is contained in these quantities is the representation in terms of overlap of light-cone wave functions (LCWFs) which are the probability amplitudes to find a given N -parton configuration in the Fock-space expansion of the hadron state [4]. In the following, we will confine our analysis to the three-quark sector, by truncating the light-cone expansion of the nucleon state to the minimal Fock-space configuration. The three-quark component of the nucleon have been studied extensively in the literature [5]-[11] in terms of quark distribution amplitudes defined as hadron-to-vacuum transition matrix elements of non-local gauge-invariant light-cone operators. Unlike these works, the authors of Refs. [12, 13] considered the wave-function amplitudes keeping full transverse-momentum dependence of partons and proposed a systematic way to enumerate independent amplitudes of a LCWF which parametrize the different orbital angular momentum components of the nucleon state. This approach consists in writing down the matrix elements of a class of three-quark light-cone quark operators which serve to define a complete set of light-cone amplitudes. These matrix elements can be simplified using color, flavor, spin and discrete symmetries [13], and at the end one finds that six amplitudes are needed to describe the three-quark sector of the nucleon LCWF. This general classification scheme can be used to obtain the overlap LCWF representation of the TMDs and GPDs, which in turn can be applied to obtain predictions within specific dynamical models of the nucleon. Here we will adopt a light-cone constituent quark model (CQM) which has been successfully applied in the calculation of the electroweak properties of the nucleon [14]. As outlined in Ref. [15], the starting point is the three-quark wave function obtained as solution of the Schrödinger-like eigenvalue equation in the instant-form dynamics. The corresponding solution in light-cone dynamics is obtained through the unitary transformation represented by product of Melosh rotations acting on the spin of the individual quarks. In particular, the instant-form wave function is constructed as a product of a momentum wave function which is spherically symmetric and invariant under permutations, and a spin-isospin wave function which is uniquely determined by SU(6) symmetry requirements. By applying the Melosh rotations, the Pauli spinors of the quarks in the nucleon rest frame are converted to the light-cone spinor. The relativistic spin effects are evident in the presence of spin-flip terms in the Melosh rotations which generate non-zero orbital angular momentum component and non-trivial correlations between spin and transverse momentum of the quarks. On the other hand, the momentum-dependent wave function keeps the original functional form, with instant-form coordinates rewritten in terms of light-cone coordinates. The explicit expressions of the light-cone amplitudes within this CQM can be found in Ref. [16], while the corresponding results for the TMDs and GPDs in the impact-parameter space will be discussed in sect. 2 and 3, respectively.

TRANSVERSE-MOMENTUM DEPENDENT DISTRIBUTIONS

SIDIS processes are described at leading order by eight TMDs, f_1^q , $f_{1T}^{\perp q}$, g_1^q , g_{1T}^q , $g_{1L}^{\perp q}$, h_1^q , $h_{1T}^{\perp q}$, and $h_{1L}^{\perp q}$, which depend on x and \mathbf{k}_\perp^2 . Among them, the Boer-Mulders

h_1^\perp [17] and the Sivers f_{1T}^\perp [18] functions are T-odd, i.e. they change sign under “naive time reversal”, which is defined as usual time reversal, but without interchange of initial and final states. Restricting the analysis to the remaining six T-even TMDs, we find the following results within our light-cone CQM [16]

$$\begin{aligned}
f_1^q(x, \mathbf{k}_\perp^2) &= N^q \int d[1]d[2]d[3] \delta(k - k_3) |\psi(\{x_i\}, \{\mathbf{k}_{\perp i}\})|^2, \\
g_{1L}^q(x, \mathbf{k}_\perp^2) &= P^q \int d[1]d[2]d[3] \delta(k - k_3) |\psi(\{x_i\}, \{\mathbf{k}_{\perp i}\})|^2 \frac{(m + xM_0)^2 - \mathbf{k}_\perp^2}{(m + xM_0)^2 + \mathbf{k}_\perp^2}, \\
g_{1T}^q(x, \mathbf{k}_\perp^2) &= P^q \int d[1]d[2]d[3] \delta(k - k_3) |\psi(\{x_i\}, \{\mathbf{k}_{\perp i}\})|^2 \frac{2M(m + xM_0)}{(m + xM_0)^2 + \mathbf{k}_\perp^2}, \\
h_1^q(x, \mathbf{k}_\perp^2) &= P^q \int d[1]d[2]d[3] \delta(k - k_3) |\psi(\{x_i\}, \{\mathbf{k}_{\perp i}\})|^2 \frac{(m + xM_0)^2}{(m + xM_0)^2 + \mathbf{k}_\perp^2}, \\
h_{1T}^{\perp q}(x, \mathbf{k}_\perp^2) &= -P^q \int d[1]d[2]d[3] \delta(k - k_3) |\psi(\{x_i\}, \{\mathbf{k}_{\perp i}\})|^2 \frac{2M^2}{(m + xM_0)^2 + \mathbf{k}_\perp^2}, \\
h_{1L}^{\perp q}(x, \mathbf{k}_\perp^2) &= -P^q \int d[1]d[2]d[3] \delta(k - k_3) |\psi(\{x_i\}, \{\mathbf{k}_{\perp i}\})|^2 \frac{2M(m + xM_0)}{(m + xM_0)^2 + \mathbf{k}_\perp^2},
\end{aligned} \tag{1}$$

where $\delta(k - k_3) = \delta(x - x_3) \delta(\mathbf{k}_\perp - \mathbf{k}_{\perp 3})$, and the integration measures are defined as

$$d[1]d[2]d[3] = dx_1 dx_2 dx_3 \delta\left(1 - \sum_{i=1}^3 x_i\right) \frac{d^2 \mathbf{k}_{\perp 1} d^2 \mathbf{k}_{\perp 2} d^2 \mathbf{k}_{\perp 3}}{[2(2\pi^3)]^2} \delta\left(\sum_{i=1}^3 \mathbf{k}_{\perp i}\right). \tag{2}$$

In Eqs. (1), the flavor dependence is given by the factors $P^u = \frac{4}{3}$, $P^d = -\frac{1}{3}$, $N^u = 2$ and $N^d = 1$, as dictated by SU(6) symmetry. A further consequence of the assumed SU(6) symmetry is the factorization in Eqs. (1) of the momentum-dependent wave function $\psi(\{x_i\}, \{\mathbf{k}_{\perp i}\})$ from the spin-factor arising from the Melosh rotations. Thanks to this factorized form one finds the following relations

$$2h_1^q(x, \mathbf{k}_\perp^2) = g_{1L}^q(x, \mathbf{k}_\perp^2) + \frac{P^q}{N^q} f_1^q(x, \mathbf{k}_\perp^2), \tag{3}$$

$$\frac{P^q}{N^q} f_1^q(x, \mathbf{k}_\perp^2) = h_1^q(x, \mathbf{k}_\perp^2) - \frac{\mathbf{k}_\perp^2}{2M^2} h_{1T}^{\perp q}(x, \mathbf{k}_\perp^2), \tag{4}$$

$$h_{1L}^{\perp q}(x, \mathbf{k}_\perp^2) = -g_{1T}^q(x, \mathbf{k}_\perp^2). \tag{5}$$

Eq. (3) is a generalization of analogous relations discussed in Ref. [19, 20] and was also rederived together with Eq. (4) in Ref. [21]. Eq. (5) was already found in the diquark spectator model of Ref. [22]. In QCD TMDs should be all independent of each other. The limitation to three valence quarks implies that out of the six TMDs f_1 , g_{1L} , g_{1T} , h_1 , h_{1T}^\perp , h_{1L}^\perp only three are linearly independent. A similar situation occurs with the bag

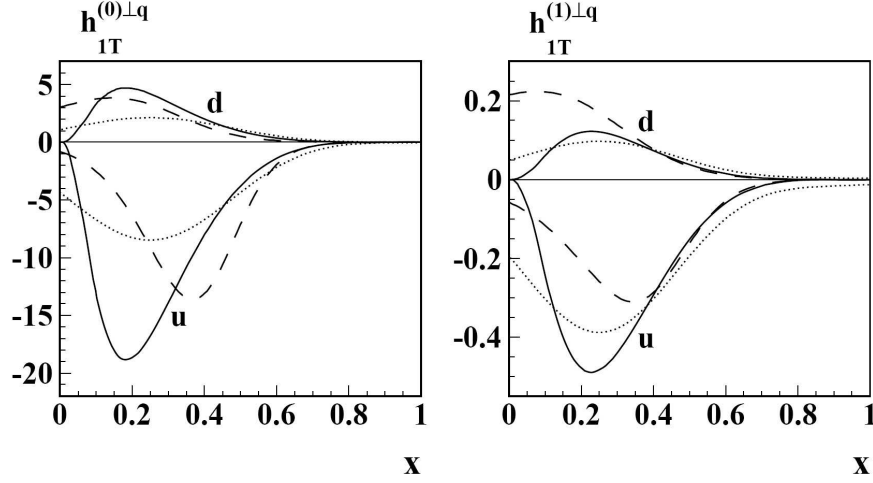


FIGURE 1. The transverse moments $h_{1T}^{(0)\perp q}(x)$ (left panel) and $h_{1T}^{(1)\perp q}(x)$ (right panel). Solid curves: results from the light-cone CQM model. Dashed curves: results from the spectator model of Ref. [22]. Dotted curves: results from the bag model.

model [21]. In the diquark spectator model of Ref. [22] the relations (3) and (4) hold only for the separate scalar and axial contributions, while Eq. (5) is verified more generally for both u and d flavors. However, this is no longer true by considering different versions of the diquark spectator model as in Refs. [23, 24]. Furthermore, combining the relations (3) and (4), one finds for the h_{1T}^{\perp} distribution

$$\frac{\mathbf{k}_{\perp}^2}{2M^2} h_{1T}^{\perp q}(x, \mathbf{k}_{\perp}^2) = g_{1L}^q(x, \mathbf{k}_{\perp}^2) - h_1^q(x, \mathbf{k}_{\perp}^2). \quad (6)$$

This result was already found in Ref. [21]. Integrating out transverse momenta and going to the non-relativistic limit where helicity and transversity distributions coincide, one finds that the first moment of h_{1T}^{\perp} vanish identically. Thus, relation (6) supports the statement that h_{1T}^{\perp} is a measure of relativistic effects. Relativity, responsible for a chiral-odd transversity distribution differing from a chiral-even helicity distribution, exhibits the chirally odd nature of h_{1T}^{\perp} . This is confirmed by the following relation that is also satisfied within our model:

$$h_{1T}^{(0)\perp q}(x) = \frac{3}{(1-x)^2} \tilde{H}_T^q(x, 0, 0), \quad (7)$$

where $\tilde{H}_T^q(x, 0, 0)$ is the forward limit of a chiral-odd generalized parton distribution occurring in the case of parton and nucleon helicity flip (see, e.g., Refs. [19, 25]) and the transverse moments of $h_{1T}^{\perp q}$ are defined as $h_{1T}^{(n)\perp q}(x) = \int d^2 k_{\perp} \left(\frac{\mathbf{k}_{\perp}^2}{2M^2} \right)^n h_{1T}^{\perp q}(x, \mathbf{k}_{\perp}^2)$. Eq. (7) was first found in Ref. [3] to hold for the scalar diquark model and in a quark target model of the nucleon.

The results for all the T-even TMDs are discussed in details in Ref. [16], and here we focus only on the distribution $h_{1T}^{\perp q}$. This distribution contributes when the quark and

nucleon helicity flip in opposite directions. It then requires an overlap between wave function components that differ by two units of orbital angular momentum, either a PP or an SD interference. While in the case of u quarks the PP and SD interference terms add with the same sign, in the case of d quarks they have opposite sign, indicating that in the present model the SU(6) relation between u and d contributions, $h_{1T}^{\perp u} = -4h_{1T}^{\perp d}$, is valid for the total result but not for the partial wave contributions. The transverse moments of $h_{1T}^{\perp q}$ are rather different in different models, as can be seen in Fig. 1 where the light-cone CQM results are compared with results of the bag model and the spectator model of Ref. [22]. This sensitivity to the adopted model suggests that the experiments planned at COMPASS, HERMES and JLab [26] could give useful insights to model the momentum dependence of the nucleon wave function.

According to Ref. [27], the distribution $h_{1T}^{\perp q}$ gives also a measure of the deviation of the nucleon shape from a sphere. This can be seen by defining a suitable spin-dependent quark density, $\hat{\rho}_{\text{RELT}}$, in a nucleon state polarized in the transverse direction \mathbf{S}_T either parallel or antiparallel to the quark-spin direction \mathbf{n} . The transverse shapes of the nucleon are then derived from the following relation:

$$\frac{\hat{\rho}_{\text{RELT}}(\mathbf{k}_{\perp}, \mathbf{n})/M}{\tilde{f}_1(\mathbf{k}_{\perp}^2)} = 1 + \frac{\tilde{h}_1(\mathbf{k}_{\perp}^2)}{\tilde{f}_1(\mathbf{k}_{\perp}^2)} \cos \phi_n + \frac{\mathbf{k}_{\perp}^2}{2M^2} \cos(2\phi - \phi_n) \frac{\tilde{h}_{1T}^{\perp}(\mathbf{k}_{\perp}^2)}{\tilde{f}_1(\mathbf{k}_{\perp}^2)}, \quad (8)$$

where ϕ is the angle between \mathbf{k}_{\perp} and \mathbf{S}_T and ϕ_n is the angle between \mathbf{n} and \mathbf{S}_T . A tilde is placed over a given quantity to define the x -integrated distributions.

The transverse shapes of the proton are shown in the Fig. 2 for \mathbf{S}_T parallel to \mathbf{n} , $\phi_n = 0$ (left column), and for \mathbf{S}_T antiparallel to \mathbf{n} , $\phi_n = \pi$ (right column). The results assuming a struck u (d) quark are shown in the upper (lower) row. In our model \tilde{f}_1^u (\tilde{f}_1^d) and \tilde{h}_1^u (\tilde{h}_1^d) are of the same (opposite) sign and similar size, so that the contribution of the first two terms on the rhs of Eq. (8) tend to cancel each other for $\phi_n = \pi$ ($\phi_n = 0$) emphasizing the role of the pretzelosity in producing deformation. For u (d) quarks the last term in Eq. (8) is negative (positive) for $\phi = \phi_n = 0$ and its size increases (reduces) with the inclusion of the D-wave. This explains the larger transverse deformation in the direction antiparallel (parallel) to \mathbf{S}_T for a struck u (d) quark, with a more significant effect in the case of the u quark.

SPIN DENSITIES IN THE IMPACT PARAMETER SPACE

When $\xi = 0$ and $x > 0$, by a two-dimensional Fourier transform to impact parameter space GPDs can be interpreted as densities of quarks with longitudinal momentum fraction x and transverse location b with respect to the nucleon center of momentum [28, 29]. Depending on the polarization of both the active quark and the parent nucleon, according to Refs. [29, 30] one defines three-dimensional densities $\rho(x, b, \lambda, \Lambda)$ and $\rho(x, b, s_T, S_T)$ representing the probability to find a quark with longitudinal momentum fraction x and transverse position b either with light-cone helicity λ ($= \pm 1$) in the nucleon with longitudinal polarization Λ ($= \pm 1$) or with transverse spin s_T in the

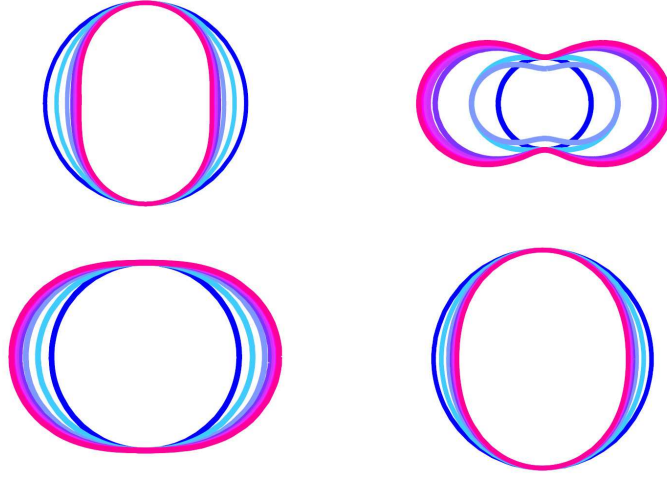


FIGURE 2. Transverse shape of the proton, $\hat{\rho}_{\text{REL}T}(\mathbf{k}_\perp, \mathbf{n})/\tilde{f}_1(\mathbf{k}_\perp^2)$, assuming a struck u (upper row) and d (lower row) quark. The horizontal axis is the direction of \mathbf{S}_\perp , while $\mathbf{n} = \hat{\mathbf{S}}_\perp$ ($\phi_n = 0$) and $\mathbf{n} = -\hat{\mathbf{S}}_\perp$ ($\phi_n = \pi$) in the left and right column, respectively. The shapes vary from the circle to the deformed shapes as k_\perp is increased from 0 to 2.0 GeV in steps of 0.25 GeV.

nucleon with transverse spin S_T . They read

$$\rho(x, b, \lambda, \Lambda) = \frac{1}{2} \left[H(x, b^2) + b^j \epsilon^{ji} S_T^i \frac{1}{M} E'(x, b^2) + \lambda \Lambda \tilde{H}(x, b^2) \right], \quad (9)$$

$$\begin{aligned} \rho(x, b, S_T, S_T) = \frac{1}{2} & \left[H(x, b^2) + S_T^i S_T^i \left(H_T(x, b^2) - \frac{1}{4M^2} \Delta_b \tilde{H}_T(x, b^2) \right) \right. \\ & + \frac{b^j \epsilon^{ji}}{M} (S_T^i E'(x, b^2) + S_T^i [E_T'(x, b^2) + 2\tilde{H}_T'(x, b^2)]) \\ & \left. + S_T^i (2b^i b^j - b^2 \delta_{ij}) S_T^j \frac{1}{M^2} \tilde{H}_T''(x, b^2) \right]. \end{aligned} \quad (10)$$

where the derivatives are defined $f' = \frac{\partial}{\partial b^2} f$, and $\Delta_b f = 4 \frac{\partial}{\partial b^2} \left(b^2 \frac{\partial}{\partial b^2} \right) f$. In Eqs. (9)-(10) there appear the Fourier transforms of the GPDs for unpolarized quarks (H and E), for longitudinally polarized quarks (\tilde{H} and \tilde{E}) and transversely polarized quarks (H_T , E_T , \tilde{H}_T , and \tilde{E}_T).

In Eq. (9) the first term with H describes the density of unpolarized quarks in the unpolarized proton. The term with E' introduces a sideways shift in such a density when the proton is transversely polarized, and the term with \tilde{H} reflects the difference in the density of quarks with helicity equal or opposite to the proton helicity.

In the three lines of Eq. (10) one may distinguish the three contributions corresponding to monopole, dipole and quadrupole structures. The unpolarized quark density $\frac{1}{2}H$ in the monopole structure is modified by the chiral-odd terms with H_T and $\Delta_b \tilde{H}_T$ when both the quark and the proton are transversely polarized. Responsible for the dipole structure is either the same chiral-even contribution with E' from the transversely polarized proton

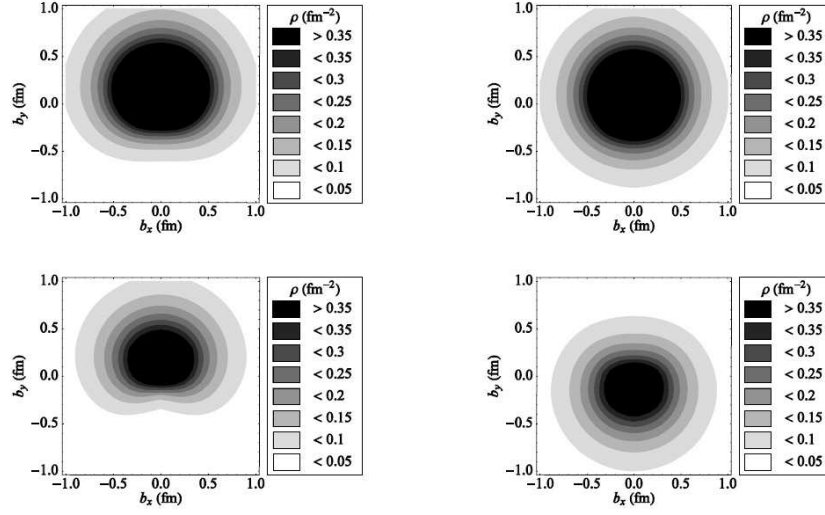


FIGURE 3. The spin-densities for (transversely) \hat{x} -polarized quarks in an unpolarized proton (left column) and for unpolarized quarks in a (transversely) \hat{x} -polarized proton (right column). The upper (lower) row corresponds to the results for up (down) quarks.

appearing in the longitudinal spin distribution (9) or the chiral-odd contribution with $E_T' + 2\tilde{H}_T'$ from the transversely polarized quarks or both. The quadrupole term with \tilde{H}_T'' is present only when both quark and proton are transversely polarized.

In the case of transversely polarized quarks in an unpolarized proton the dipole contribution introduces a large distortion perpendicular to both the quark spin and the momentum of the proton, as shown in the left column of Fig. 3. Evidently, quarks in this situation also have a transverse component of orbital angular momentum. This effect has been related [31, 32] to a nonvanishing Boer-Mulders function [17] h_1^\perp which describes the correlation between intrinsic transverse momentum and transverse spin of quarks. Such a distortion reflects the large value of the anomalous tensor magnetic moment κ_T for both flavors. Here, $\kappa_T^u = 3.98$ and $\kappa_T^d = 2.60$, to be compared with the values $\kappa_T^u \approx 3.0$ and $\kappa_T^d \approx 1.9$ of Ref. [33] due to a positive combination $E_T + 2\tilde{H}_T$. Since $\kappa_T \sim -h_1^\perp$, the present results confirm the conjecture that h_1^\perp is large and negative both for up and down quarks [31, 32].

As also noticed in Refs. [28, 33] the large anomalous magnetic moments $\kappa^{u,d}$ are responsible for the dipole distortion produced in the case of unpolarized quarks in transversely polarized nucleons (right column of Fig. 3). With the present model, $\kappa^u = 1.86$ and $\kappa^d = -1.57$, to be compared with the values $\kappa^u = 1.673$ and $\kappa^d = -2.033$ derived from data. This effect can serve as a dynamical explanation of a nonvanishing Sivers function [18] f_{1T}^\perp which measures the correlation between the intrinsic quark transverse momentum and the transverse nucleon spin. The present results, with the opposite shift of up and down quark spin distributions imply an opposite sign of f_{1T}^\perp for up and down quarks [34] as confirmed by the recent observation of the HERMES collaboration [35]. The results in Fig. 3 are also in qualitative agreement with those

obtained in lattice calculations [33].

Finally, we refer to [25, 36] for the light-cone CQM results of the densities with more complex spin-configurations with transverse polarization of both the quark as well as the proton.

ACKNOWLEDGMENTS

It is a pleasure for me to thank my collaborators who participated in different works referred to in this paper: S. Boffi, S. Cazzaniga, and M. Pincetti.

REFERENCES

1. P.J. Mulders, R.D. Tangerman, Nucl. Phys. **B 461**, 197 (1996); Erratum-*ibid.* **B 484**, 538 (1997).
2. X. Ji, Ann. Rev. Nucl. Part. Sci. **54**, 413 (2004).
3. S. Meissner, A. Metz, and K. Goeke, Phys. Rev. **D 76**, 034002 (2007); K. Goeke, A. Metz, M. Schlegel, arXiv:0805.3165; arXiv:0710.5846.
4. S.J. Brodsky, H.-Ch. Pauli, S.S. Pinsky, Phys. Rep. **301**, 299 (1998).
5. G.P. Lepage, S.J. Brodsky, Phys. Rev. **D 22**, 2157 (1980).
6. V. L. Chernyak and A. R. Zhitnitsky, Phys. Rep. **112**, 173 (1984).
7. I. D. King and C. T. Sachrajda, Nucl. Phys. **B 279**, 785 (1987).
8. V. L. Chernyak, A. A. Ogloblin, and I. R. Zhitnitsky, Z. Phys. **C 42**, 583 (1989).
9. V. M. Braun, et al., Nucl. Phys. **B 553**, 355 (1999).
10. V. Braun, *et al.*, Nucl. Phys. **B 589**, 381 (2000); Erratum-*ibid.* **B 607**, 433 (2001).
11. N.G. Stefanis, Eur. Phys. J. direct **C 7**, 1 (1999).
12. M. Burkardt, X. Ji, F. Yuan, Phys. Lett. **B 545**, 345 (2002).
13. X. Ji, J.-P. Ma and F. Yuan, Nucl. Phys. **B 652**, 383 (2003); Eur. Phys. J. **C 33**, 75 (2004); Phys. Rev. Lett. **90**, 241601 (2003).
14. B. Pasquini, and S. Boffi, Phys. Rev. **D 76**, 074011 (2007); Phys. Rev. **D 73**, 094001 (2006).
15. S. Boffi, B. Pasquini and M. Traini, Nucl. Phys. **B 649**, 243 (2003); Nucl. Phys. **B 680**, 147 (2004).
16. B. Pasquini, S. Cazzaniga, and S. Boffi, arXiv:0806.2298.
17. D. Boer, P.J. Mulders, Phys. Rev. **D 57**, 5780 (1998).
18. D.W. Sivers, Phys. Rev. **D 41**, 83 (1990).
19. B. Pasquini, M. Pincetti, and S. Boffi, Phys. Rev. **D 72**, 094029 (2005).
20. B. Pasquini, M. Pincetti, and S. Boffi, Phys. Rev. **D 76**, 034020 (2007).
21. H. Avakian, A. V. Efremov, P. Schweitzer, F. Yuan, arXiv:0805.3355 [hep-ph].
22. R. Jakob, P.J. Mulders, and J. Rodrigues, Nucl. Phys. **A 626**, 937 (1997).
23. A. Bacchetta, F. Conti, and M. Radici, e-Print: arXiv:0807.0323 [hep-ph].
24. L.P. Gamberg, G.R. Goldstein, and M. Schlegel, Phys. Rev. **D 77**, 094016 (2008).
25. S. Boffi and B. Pasquini, Rivista Nuovo Cim. **30**, 387 (2007).
26. H. Avakian, *et al.*, JLab LOI 12-06-108 (2008); JLab E05-113; JLab PR12-07-107.
27. G.A. Miller, Phys. Rev. **C 76**, 065209 (2007).
28. M. Burkardt, Phys. Rev. **D 62**, 071503 (2000); (E) Phys. Rev. **D 66**, 119903 (2002).
29. M. Burkardt, Int. J. Mod. Phys. **A 18**, 173 (2003).
30. M. Diehl, Ph. Hägler, Eur. J. Phys. **C 44**, 87 (2005).
31. M. Burkardt, Phys. Rev. **D 72**, 094020 (2005).
32. M. Burkardt, B. Hannafious, Phys. Lett. **B 568**, 130 (2008).
33. M. Göckeler, *et al.* (QCDSF/UKQCD Collaboration), Phys. Rev. Lett. **98**, 222001 (2007).
34. M. Burkardt, Phys. Rev. **D 66**, 114005 (2002); M. Burkardt, Nucl. Phys. **A 735**, 185 (2004).
35. A. Airapetian *et al.* (Hermes Collaboration), Phys. Rev. Lett. **94**, 012002 (2005).
36. B. Pasquini, and S. Boffi, Phys. Lett. **B 653**, 23 (2007).